Influence of rheological behavior of nanofluid on heat transfer

ADNAN RAJKOTWALA AND JYOTIRMAY BANERJEE*

Department of Mechanical Engineering

National Institute of Technology

Surat (Gujarat) - 395007

INDIA

jbaner@med.svnit.ac.in http://www.svnit.ac.in/deptt/med/mywebpge.htm

Abstract: - The influence of rheological behavior of nanofluid on heat transfer is established. A comparative analysis is presented for heat transfer behavior of Newtonian and non-Newtonian model of nanofluid for natural convection. Ostwald–de Waele model for non-Newtonian fluid is used for calculating the shear stresses from the velocity gradients. Brinkmann model is used for incorporating the influence of volume fraction on viscosity for Newtonian model. The numerical analysis is presented for Rayleigh number (Ra) in the range of 10^4 to 10^6 and nanoparticle volume fraction (ϕ) in the range of 0.05% to 5%. For non-Newtonian model, a reduction in the average Nusselt number is observed with increase in volume fraction (ϕ) for a particular Rayleigh number. On the other hand, augmentation of Nusselt number is observed for Newtonian model. It is also observed that heat transfer rate increases with the increase in Rayleigh number for both the cases, though the augmentation in case of Newtonian model is more compared to Non-Newtonian model.

Keywords: - Nanofluid, natural convection, non-Newtonian fluid, Brownian motion.

Nomenclature

Principal symbols

c_p	specific heat, J/kg K
Gr	Grashof number, $g\beta_f \Delta T L^3/\nu_f^2$
g	acceleration due to gravity, m/s^2
h,l	height and width of domain, m
k_b	Boltzmann constant
k	thermal conductivity, W/mK
m, n	the respective consistency and fluid behaviour index parameters
Nu_y	local Nusselt number of the hot wall
$\overline{Nu}$	average Nusselt number of the hot wall
p	pressure, N/m^2
P	dimensionless pressure
Pr	Prandtl number of the fluid, ν_f/α_f
Pe	Peclet number
Ra	Rayleigh number, GrPr
T_H, T_C	temperature of the heat source and sink respectively
u, v	velocity components in x and y directions respectively
U, V	dimensionless velocities
x, y	horizontal and vertical coordinates respectively
X, Y	dimensionless horizontal and vertical coordinates respectively
d_p	diameter of the nanoparticles, m
A	area, m^2
u_p	Brownian velocity, m/s

Greek symbols

α	thermal diffusivity, m^2/s
β	thermal expansion coefficient, 1/K
ϕ	solid volume fraction
μ	dynamic viscosity, Ns/m^2
ν	kinematic viscosity, m^2/s
ρ	density, kg/m^3
θ	dimensionless temperature
Ψ	dimensionless stream function
τ	the stress tensor
$\dot{\gamma}$	the symmetric rate of deformation tensor

Subscripts

eff	effective
f	fluid
0	at reference state
s	solid
nf	nanofluid

1. Introduction

Heat transfer characteristic of nanofluid depends on the thermo physical properties primarily viscosity, thermal conductivity, specific heat and density. To model the viscosity of nanofluid, several researchers have studied the rheology of nanofluid. While some researchers believe that nanofluid behaves as Newtonian fluid [1-2] others observed non-Newtonian behaviour [3-4]. As a part of International Nanofluid Property Benchmark Exercise (INPBE), a unified effort was made to study the rheology of nanofluids [5]. Both Newtonian and non-Newtonian behavior of nanofluid was observed in this study. Chen *et al.* [6] provided some explanation for this by stating that shear thinning behaviour of the nanofluid depends on particle volume fraction, range of the shear rate and viscosity of the base fluid. For volume fraction, $\phi < 0.001$, there is no shear thinning; for $\phi < 0.05$, there is shear thinning under low shear rates and for $\phi > 0.05$, a shear thinning behaviour is expected for all range of shear rates. Particle aggregation also has an effect on the non-Newtonian behavior of nanofluid [3]. Also a detailed rheological analysis by Chen and Ding [7] shows that nanofluid can exhibit either or both Newtonian and non-Newtonian behavior depending on particle size and shape, particle concentration, base liquid viscosity and solution chemistry.

Owing to the uncertainty in rheological behavior of nanofluids, a comparative study of its heat transfer behavior for Newtonian and non-Newtonian model is important. In the present work a comparative analysis of Newtonian and non-Newtonian model of nanofluid is presented for heat transfer in natural convection. This is because in case of forced convection, the shear stresses are significantly higher due to external pressure and thus external pressure nullifies the effect of non-Newtonian behaviour caused due to the addition of nano-particles [8].

Nanofluid considered for the present analysis is copper-water nanofluid. Copper (Cu) is selected because of its high thermal conductivity which gives a magnified analysis of the heat transfer behavior compared to CuO, Al_2O_3 and other nano particles. Nanofluids with low viscous base fluids are more likely to exhibit non-Newtonian behavior than those made of highly viscous base fluids (e.g. ethylene glycol and propylene glycol) [7]. Also shear thinning is observed at higher shear rates for less viscous base fluids like water [6]. Thus water based nanofluids are expected to behave as non-Newtonian fluid even at low particle concentration. At higher Rayleigh number (Ra), velocity gradients are higher thereby generating higher shear rates. Thus water based nanofluids are also expected to behave as non-Newtonian fluid at higher Rayleigh number (Ra). The shear dependence of viscosity of very dilute nanofluids is negligible, while nanofluids with relatively high concentration are more likely to exhibit shear thinning behavior [7]. Thus for the present analysis volume fraction of nanoparticles in the range of 1% to 5% is considered.

Experimental investigations had shown that the thermal conductivity of nanofluid is influenced by the random and irregular movement of the particles in the base fluid since these motions increase the energy exchange rates in fluids. Buongiorno [9] proposed a mathematical model to capture the nanoparticle/base fluid slip by treating nanofluid as two-component mixture. He considered seven slip mechanisms: inertia, Brownian diffusion, thermophoresis, diffusiophoresis, Magnus effect, fluid drainage, and gravity. He proved that Brownian motion and thermophoresis are the main mechanisms for the relative slip velocity between nanoparticles and base fluid. Koo and Kleinstreuer [10] had however demonstrated that Brownian motion has more impact on thermal properties than thermophoresis. Brownian motion of nano-particles can bring a contribution to thermal conductivity by two ways: directly via nano-particle diffusion and indirectly via intensification of micro-convection of fluid around separate nano-particles. Jang and Choi [11] were the first to propose a model based on Brownian motion induced nano-convection. Kumar *et al*. [12] proposed a model based on heat flow through conduction in base fluid and solid particles and heat flow due to Brownian motion. However, later Keblinski and Cahill [13] pointed out that the treatment of Brownian motion by Kumar *et al*. [12] required an unphysical assumption of the nano-particle mean free path equal to 1 cm and thus over-estimated the contribution of Brownian motion to heat flow. Patel *et al*. [14] improved the model proposed by Kumar *et al.* [12] by incorporating the effect of micro-convection due to particle movement. The model takes into account the effect of the Brownian motion and particle size (through an increase in the specific area of the nanoparticles). The model is semi-empirical in nature and the constant "C" proposed by the authors is of the order of 10^4. Recently some researchers have proposed a combination of static and dynamic models available in literature [15-17]. The model proposed by Patel *et al.* [14] is considered in the present study for

calculating thermal conductivity of nanofluid because: (i) It includes the effect of micro-convection exclusively which in the present state of art is considered to be the most probable reason for rise in thermal conductivity and (ii) Though it is semi-empirical, the value of constant 'C' is such that it matches exactly with the experimental results of Xuan and Li [18] for the copper water nanofluid.

The present work is thus a numerical analysis for buoyancy driven flow of Copper-water nanofluid in a square cavity for both non-Newtonian and Newtonian model. The micro-convection model of Patel *et al.* [14] is used for calculating thermal conductivity. Brinkmann model [19] is used to calculate the viscosity of Newtonian fluid and Ostwald-de Waele model [20] (two parameter power law model) is used for non-Newtonian behavior of fluid. The governing conservation equations are derived in terms of stream function and vorticity and solved implicitly.

2. Mathematical Model

2.1 Models for calculating properties of nanofluid

Xuan and Roetzel [21] considered nanofluids as a conventional single-phase fluid assuming a no-slip condition between the particles and the base fluid. The effective thermo-physical properties were calculated as function of properties of both constituents and their respective concentrations. Thus, all equations of conservation were directly extended to nanofluids. The major properties affecting the flow and heat transfer are viscosity, heat capacity, density, thermal expansion co-efficient and thermal conductivity. These properties are calculated for the nanofluids using the suitable models proposed by different researchers. The effective density (ρ_{nf}) and heat capacity ($(\rho c_p)_{nf}$)of the nanofluid in the present work are calculated from the classical formulation for two phase mixure proposed by Xuan and Roetzel [21] :

$$\rho_{nf} = (1-\phi)\rho_f + \phi\rho_s \quad (1)$$

$$\left(\rho c_p\right)_{nf} = (1-\phi)\left(\rho c_p\right)_f + \phi\left(\rho c_p\right)_s \quad (2)$$

Similarly effective thermal expansion coefficient is calculated by

$$\rho_{nf}\beta_{eff} = (1-\phi)(\rho\beta)_f + \phi(\rho\beta)_s \quad (3)$$

The model proposed by Patel *et al.* [14] is considered in the present work for calculating the effective thermal conductivity because it includes the effect of micro-convection in addition to conduction through liquid and conduction through solid and thus defines the change of thermal conductivity with the change in temperature. Here, it is assumed that the liquid medium and the nanoparticles are in local thermal equilibrium at each location, and so the temperature gradients in liquid and solid phases are the same. Patel *et al.* [14] assumed only one-directional heat transfer in their model. Thus particle movement (by Brownian motion) in one direction only is responsible for increasing the heat transfer [14].

$$\frac{k_{eff}}{k_f} = 1 + \frac{k_p}{k_f}\frac{A_p}{A_f} + ck_p Pe + \frac{A_p}{k_f A_f} \quad (4)$$

where $\frac{A_p}{A_f} = \frac{d_f}{d_p}\frac{\phi}{1-\phi}$ (5)

Here, the Peclet number is defined as $\mathrm{Pe} = \frac{u_p d_p}{\alpha_f}$ and the Brownian motion velocity given by $u_p = \frac{2k_b T}{\pi\mu_f d_p^2}$; where k_b is the Boltzmann constant, μ_f is the dynamic viscosity of the base fluid, d_p is the diameter of the nano particle, d_f is the size of the molecules of base fluid and α_f is the thermal diffusivity of the base fluid.

The variation of viscosity with particle volume fraction (ϕ) is given by Brinkmann model [19] for Newtonian nanofluid. For the non-Newtonian fluid, the variation of the viscosity does not depend on any direct co-relation but depends on the shear rates (which are influenced by velocity field) and thus indirectly incorporate the effect of volume fraction on viscosity. The Ostwald-de Waele model [20] is used for estimation of viscosity and is discussed in the next section.

2.2 Governing equations for flow and heat transfer

The governing equations for two dimensional, steady, incompressible, single phase model of the thermally driven nanofluid are:

Continuity equation:

$$\frac{\partial \mathrm{u}}{\partial \mathrm{x}} + \frac{\partial \mathrm{v}}{\partial \mathrm{y}} = 0 \quad (6)$$

X-Momentum equation:

$$\rho_{nf}\left(u\frac{\partial u}{\partial x}+v\frac{\partial u}{\partial y}\right)=-\frac{\partial p}{\partial x}-\left[\frac{\partial \tau_{xx}}{\partial x}+\frac{\partial \tau_{yx}}{\partial y}\right] \quad (7)$$

Y-Momentum equation:

$$\rho_{nf}\left(u\frac{\partial v}{\partial x}+v\frac{\partial v}{\partial y}\right)=-\frac{\partial p}{\partial y}-\left[\frac{\partial \tau_{xy}}{\partial x}+\frac{\partial \tau_{yy}}{\partial y}\right]+\rho_{nf}\beta_{eff}\,g(T-T_c) \quad (8)$$

Energy equation:

$$\left(u\frac{\partial T}{\partial x}+v\frac{\partial T}{\partial y}\right)=\alpha_{nf}\left[\frac{\partial^2 T}{\partial x^2}+\frac{\partial^2 T}{\partial y^2}\right] \quad (9)$$

where $\alpha_{nf}=\frac{k_{nf}}{(\rho c_p)_{nf}}$ (10)

For non-Newtonian model of nanofluid

The relationship between the shear rate and shear stress is given by Ostwald model [20]:

$$\tau=-m\left[\left|\sqrt{\frac{1}{2}}(\dot{\gamma}.\dot{\gamma})\right|^{n-1}\right]\dot{\gamma} \quad (11)$$

where

$$\frac{1}{2}(\dot{\gamma}.\dot{\gamma})=2\left\{\left(\frac{\partial u}{\partial x}\right)^2+\left(\frac{\partial v}{\partial y}\right)^2\right\}+\left(\frac{\partial v}{\partial x}+\frac{\partial u}{\partial y}\right)^2 \quad (12)$$

Thus the stress tensors of equation (2) and (3) can be written as

$$\tau_{xx}=-2\left\{m\left[\left|\left[2\left\{\left(\frac{\partial u}{\partial x}\right)^2+\left(\frac{\partial v}{\partial y}\right)^2\right\}+\left(\frac{\partial v}{\partial x}+\frac{\partial u}{\partial y}\right)^2\right]^{\frac{1}{2}}\right|^{n-1}\right]\right\}\left(\frac{\partial u}{\partial x}\right) \quad (13)$$

$$\tau_{xy}=\tau_{yx}=-\left\{m\left[\left|\left[2\left\{\left(\frac{\partial u}{\partial x}\right)^2+\left(\frac{\partial v}{\partial y}\right)^2\right\}+\left(\frac{\partial v}{\partial x}+\frac{\partial u}{\partial y}\right)^2\right]^{\frac{1}{2}}\right|^{n-1}\right]\right\}\left(\frac{\partial u}{\partial y}+\frac{\partial v}{\partial x}\right) \quad (14)$$

$$\tau_{yy}=-2\left\{m\left[\left|\left[2\left\{\left(\frac{\partial u}{\partial x}\right)^2+\left(\frac{\partial v}{\partial y}\right)^2\right\}+\left(\frac{\partial v}{\partial x}+\frac{\partial u}{\partial y}\right)^2\right]^{\frac{1}{2}}\right|^{n-1}\right]\right\}\left(\frac{\partial v}{\partial y}\right) \quad (15)$$

where *m* and *n* are empirical constants that depend on the volume fraction ϕ and type of the nanofluid. The values given in the table 1 were interpolated by Santra *et al.* [22] from the experimental results of Putra *et al.* [23] and are used in the present work for Cu-water nanofluid. The decreasing value of *n* indicates the shear thinning behavior.

Solid volume fraction (ϕ) (%)	*m* (Nsec^n m^{-2})	*n*
0.5	0.0187	0.880
1	0.00230	0.830
2	0.00347	0.730
3	0.00535	0.625
4	0.00750	0.540
5	0.01020	0.460

Table 1 Values of fluid index behaviour parameter in equations (13), (14) and (15).

For Newtonian model of nanofluid

Substituting $m=\mu_{nf}$ and $n=1$ equations (13-15) reduces to shear stress relations for Newtonian fluid. The viscosity of the nanofluid for Newtonian model is given by Brinkmann model [19] as:

$$\mu_{nf}=\frac{\mu_f}{(1-\phi)^{2.5}}.$$

2.3 Non dimensional form of the governing equations

The governing equations are non-dimensionalized using the following scales:

$$X=\frac{x}{h},\quad Y=\frac{y}{h},\quad U=\frac{uh}{\alpha},\quad V=\frac{vh}{\alpha}$$

$$P=\frac{(p-p_0)h^2}{\rho_{nf}\alpha^2},\quad \theta=\frac{T-T_C}{T_H-T_C},\quad \mathrm{Gr}=\frac{g\beta_f(T_H-T_C)h^3}{\nu_f^2}$$

and $\mathrm{Pr}=\frac{\nu_f}{\alpha_f}$

where non-dimensional terms Gr and Pr are Grashof number and Prandtl number respectively corresponding to the properties of the base fluid. The non-dimensional equations are:

Non-dimensional continuity equation:

$$\frac{\partial U}{\partial X}+\frac{\partial V}{\partial Y}=0 \quad (16)$$

Non-dimensional X-momentum equation:

$$U\frac{\partial U}{\partial X}+V\frac{\partial U}{\partial Y}=-\frac{\partial P}{\partial X}+\frac{\mu_{app}}{\rho_{nf}\,\alpha_f}\left[\frac{\partial^2 U}{\partial X^2}+\frac{\partial^2 U}{\partial Y^2}\right] \quad (17)$$

Non-dimensional Y-momentum equation:

$$U\frac{\partial V}{\partial X}+V\frac{\partial V}{\partial Y}=-\frac{\partial P}{\partial Y}+\frac{\mu_{app}}{\rho_{nf}\,\alpha_f}\left[\frac{\partial^2 V}{\partial X^2}+\frac{\partial^2 V}{\partial Y^2}\right]+ \mathrm{GrPr}^2\frac{\beta_{eff}}{\beta_f}\theta \quad (18)$$

Non-dimensional energy equation:

$$U\frac{\partial \theta}{\partial X}+V\frac{\partial \theta}{\partial Y}=\frac{\alpha_{nf}}{\alpha_f}\left[\frac{\partial^2 \theta}{\partial X^2}+\frac{\partial^2 \theta}{\partial Y^2}\right] \quad (19)$$

In the equations (16) and (17), the term μ_{app} is given by:

For non-Newtonian approach

$$\mu_{app}=m\left(\frac{\alpha_f}{h^2}\right)^{n-1}\left|\left[2\left\{\left(\frac{\partial U}{\partial X}\right)^2+\left(\frac{\partial V}{\partial Y}\right)^2\right\}+\left(\frac{\partial V}{\partial X}+\frac{\partial U}{\partial Y}\right)^2\right]^{\frac{1}{2}}\right|^{n-1} \quad (20)$$

For Newtonian approach

$$\mu_{app}=\mu_{nf} \quad (21)$$

Nusselt number calculation

The local Nusselt number is calculated as:

$$Nu_Y=-\frac{k_{eff}}{k_f}\frac{\partial \theta}{\partial X}\Big|_{X=0,Y} \quad (22)$$

The average Nusselt number over the hot surface is given by

$$\overline{Nu}=\int_0^1 Nu_Y.dY \quad (23)$$

3. Numerical Method

The governing equations are solved in terms of the stream function and vorticity using fully implicit time marching algorithm. Second order upwind scheme is used for the spatial discretization of convective terms. The discretized equations are solved iteratively by Gauss-Seidal Successive-Over-Relaxation method using proper under relaxation. Also the variables k_{eff} and μ_{app} are underrelaxed to decrease the effect of non-linearity resulting due to them. A convergence criterion of 10^{-7} is set for all the physical variables.

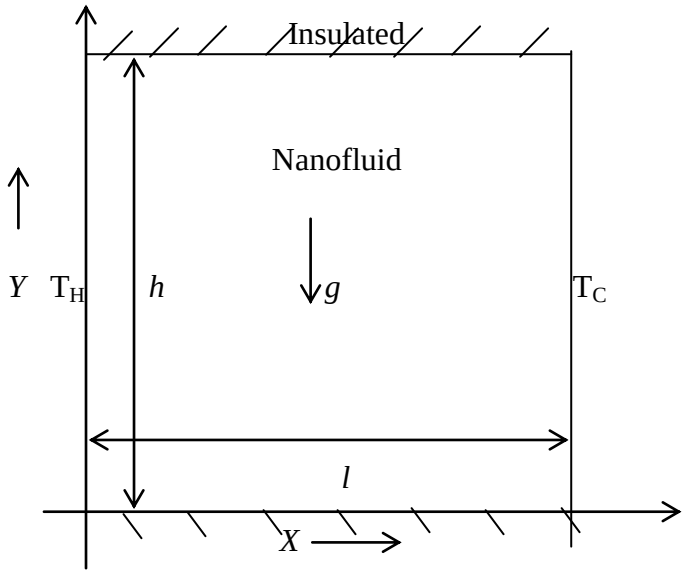

Fig. 1 Physical model of the problem

4. Problem Definition

Buoyancy driven flow of nanofluid in a two-dimensional square enclosure is considered for analysis as shown in figure 1. Copper particles of 100 nm diameter are considered as nanoparticles and water as the base fluid. Properties of water and copper at 20^0C are tabulated in table 2. Nanofluid is assumed to be incompressible. The side walls of the enclosure are kept at constant temperature T_H (30^0C) and T_C (20^0C) where T_C is taken as reference temperature. The top and bottom walls are considered to be insulated i.e. non-conducting. The boundaries have no-slip tangential and zero normal velocity boundary condition. Nanoparticles are of same shape and size. Density gradients are considered only in the buoyancy force through Boussinesq approximation.

Property	Fluid (water)	Solid (copper)
$C_p\ (J/kg\,K)$	4181.80	383.1
$\rho\ (kg/m^3)$	1000.52	8954.0
$k\ (W/m\,K)$	0.597	386.0
$\beta\ (K^{-1})$	210.0 x 10^{-6}	51.0 x 10^{-6}

Table 2 Thermophysical properties of Copper and water at 20^0C

5. Code Validation and Grid Independence

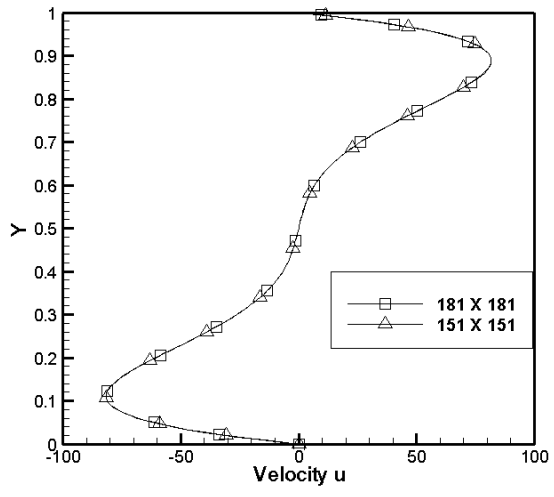

(a)

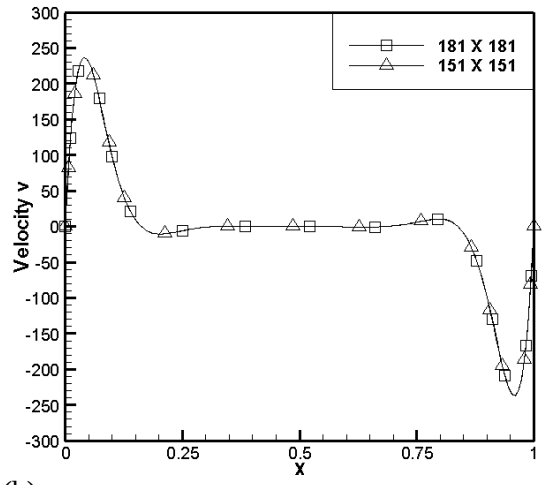

(b)

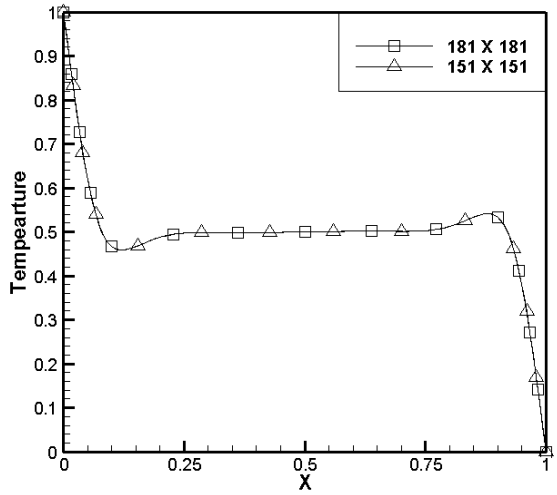

(c)

Fig. 2 Grid independence study

The code is validated by comparing the Nusselt number (Nu) obtained by the present computation with the results reported by different authors. The comparison for different Rayleigh number is shown in table 3. The horizontal velocity u, vertical velocity v and temperature T along the horizontal centerline for uniform grid size of 151 ×151 and 181 × 181 in the domain are shown in the figure 2. The solutions obtained by 151 × 151 and 181 ×181 grids have negligible difference. Hence all the solutions reported here are obtained using uniform grid of size 151 × 151.

Rayleigh number (Ra)	Present	De Vahl Davis [24]	Khanafer [25]	Fusegi [26]
10^4	2.237	2.243	2.245	2.302
10^5	4.539	4.519	4.522	4.646
10^6	8.834	8.799	8.826	9.012

Table 3 Validation of the results by comparing Nusselt number (Nu) for different Raleigh number (Ra)

6. Results and Discussions

The analysis of flow and heat transfer for copper-water nanofluid in the range of Ra = 10^4 to 10^6 and volume fraction ϕ = 0% to 5% is presented here. Prandtl number of water at 20^0C is taken as 7.02. The value of constant 'C' appearing in the thermal conductivity model is taken as 2.5×10^4 [14].

6.1 Influence of solid volume fraction

Figure 3 shows the variation of horizontal velocity along the vertical centerline, vertical velocity along the horizontal centerline and temperature along the horizontal centerline of the cavity for both Newtonian and non-Newtonian model of the flow

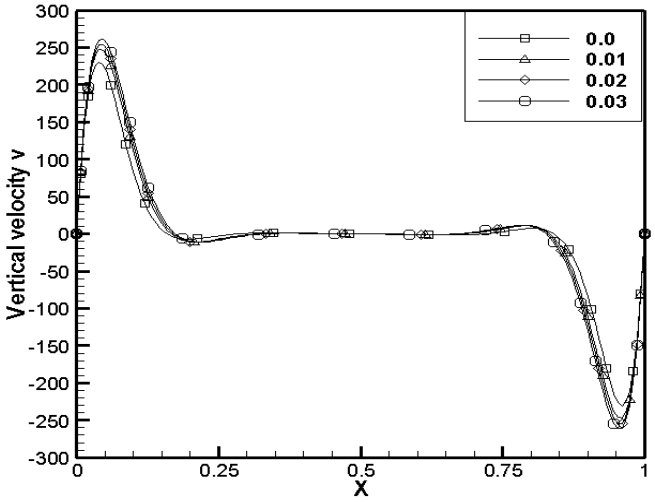

(a)

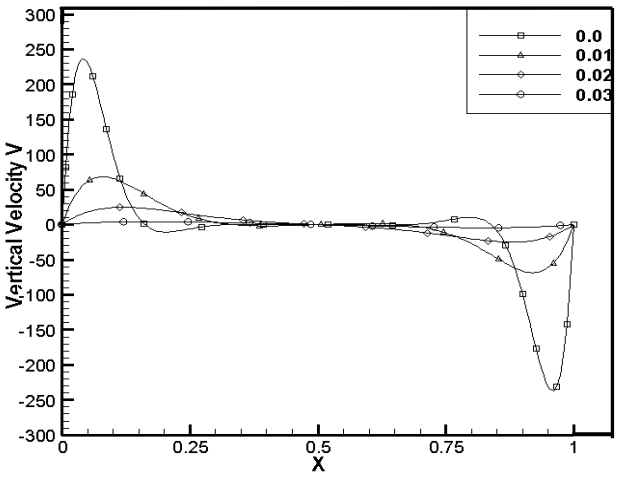

(d)

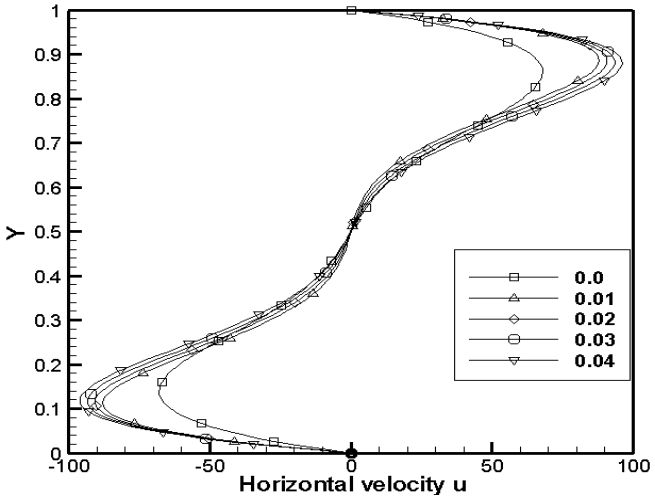

(b)

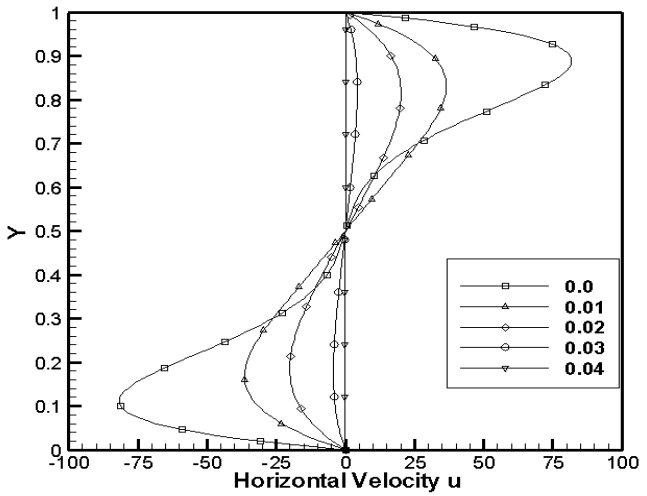

(e)

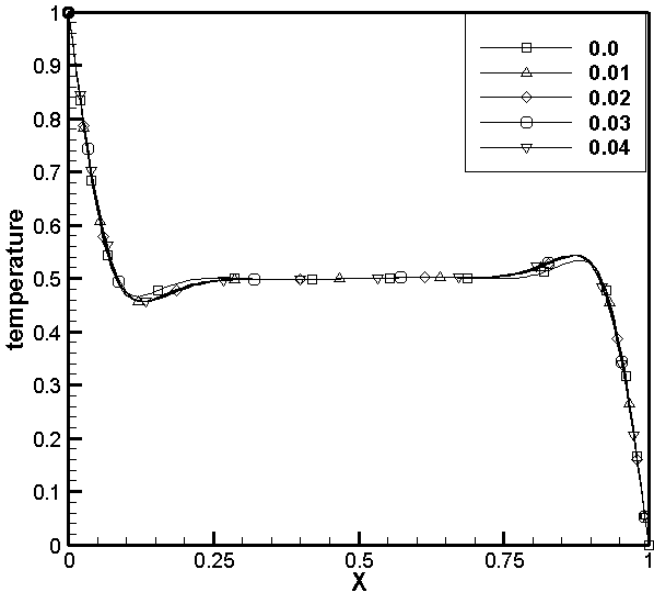

(c)

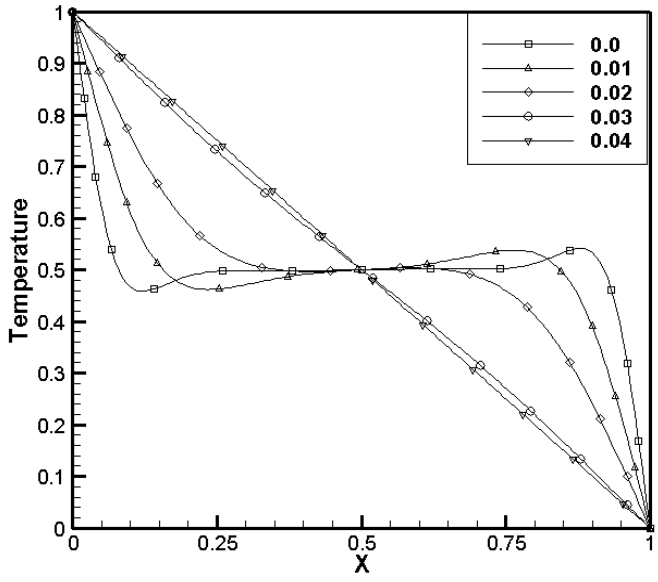

(f)

Fig. 3 (a, d) Variation of vertical velocity (v) with vertical direction (y) at x= 0.5; (b, e) variation of horizontal velocity with x at y = 0.5; (c, f) variation of temperature with x at y = 0.5 for Newtonian model (left) and non-Newtonian model (right) of nanofluid at $Ra = 10^6$.

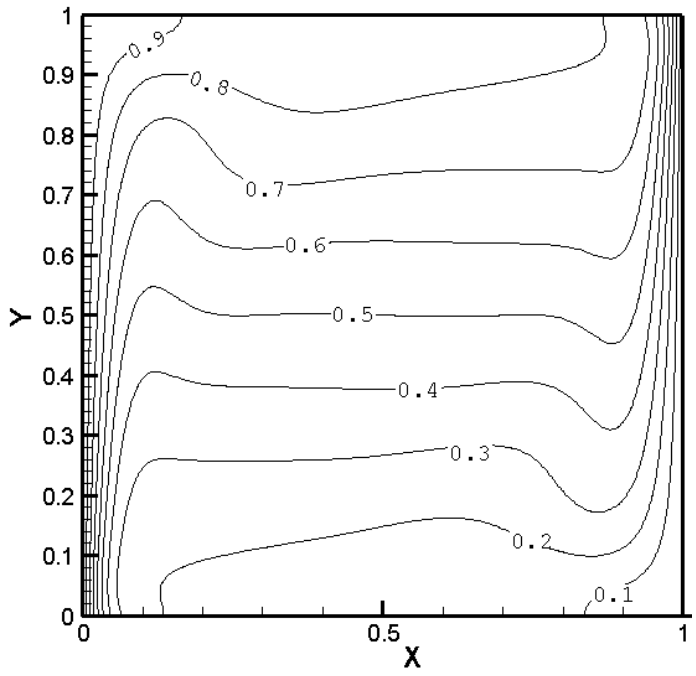

(a)

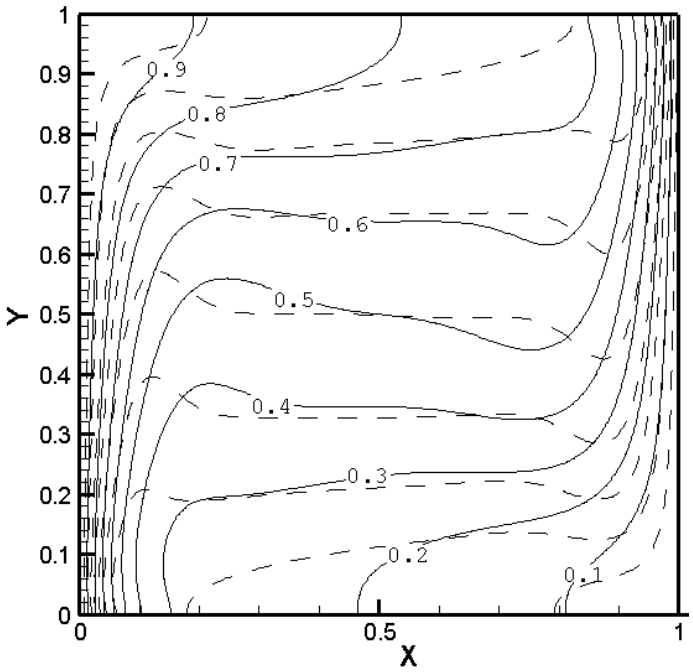

(b)

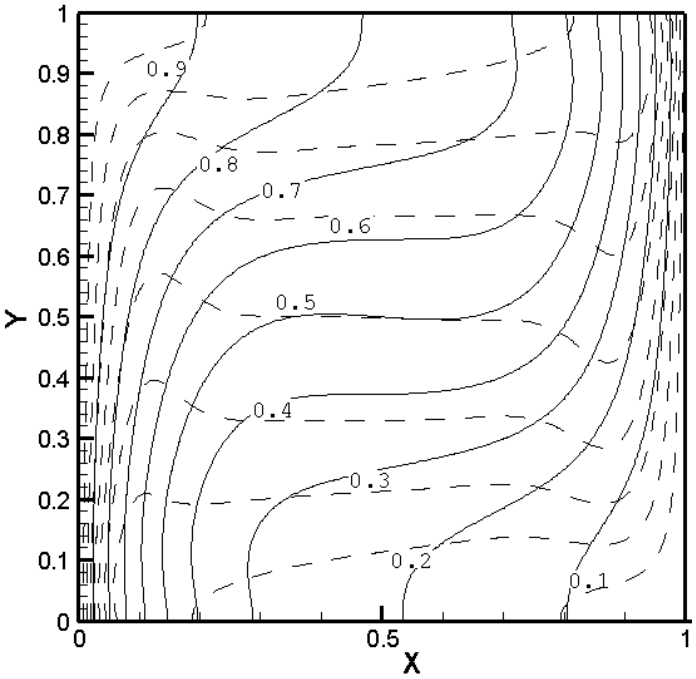

(c)

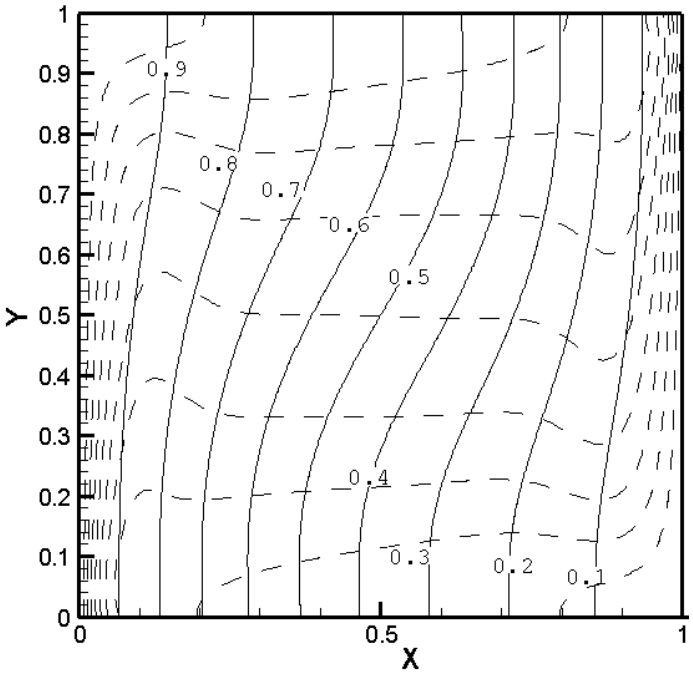

(d)

Fig. 4 Isotherms for Newtonian (dashed lines) and non-Newtonian nanofluid at $Ra = 10^6$; (a) $\phi = 0\%$, (b) $\phi = 1\%$, (c) $\phi = 2\%$ and (d) $\phi = 3\%$

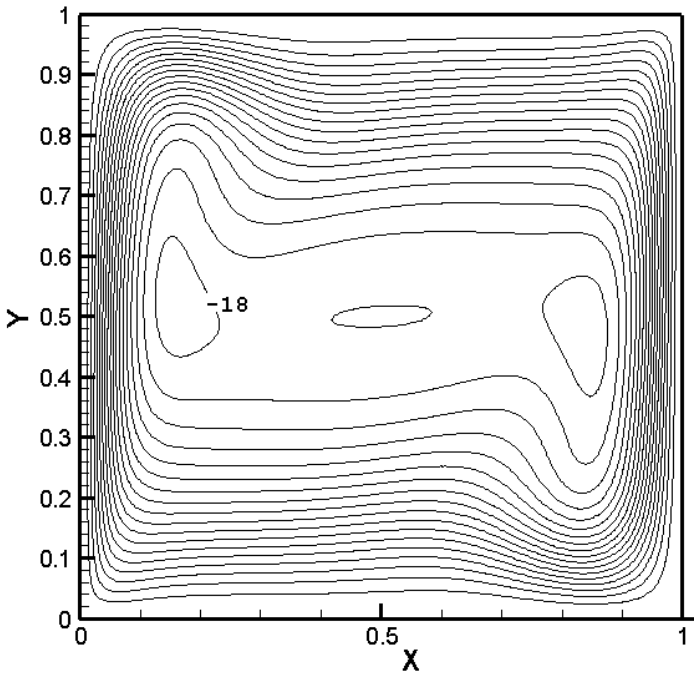

(a)

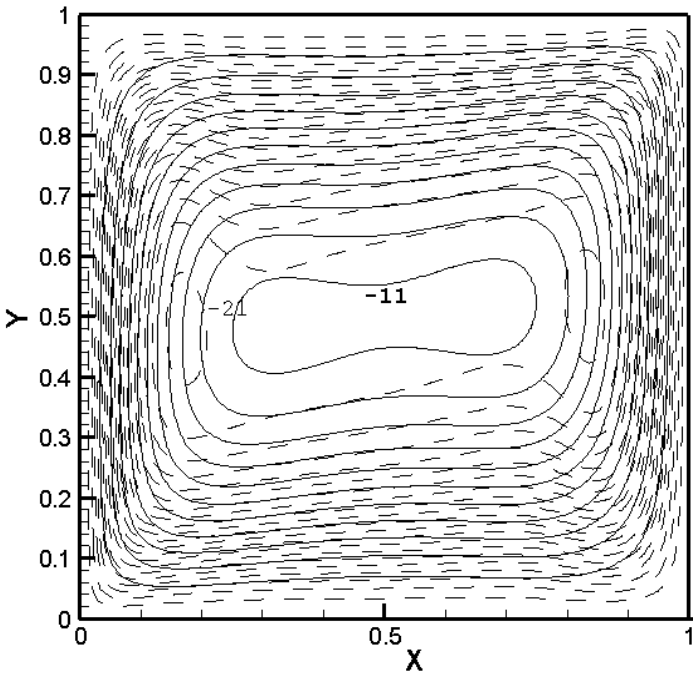

(b)

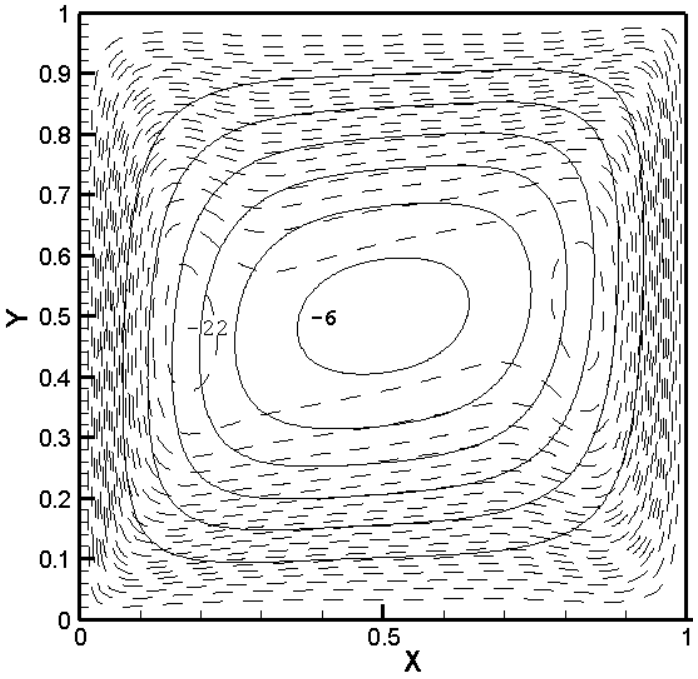

(c)

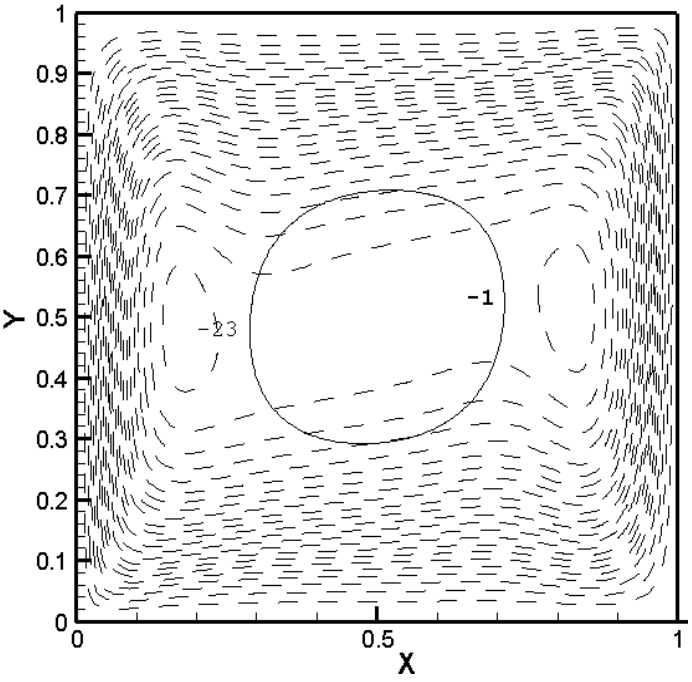

(d)

Fig. 5 Stream lines for Newtonian (dashed lines) and non-Newtonian nanofluid at $Ra = 10^6$; (a) $\phi = 0\%$, (b) $\phi = 1\%$, (c) $\phi = 2\%$ and (d) $\phi = 3\%$

for various values of volume fractions and at a fixed value of Rayleigh number. From figure 3(a), it can be observed that the vertical velocity near the hot wall is high. This is because the fluid becomes lighter when it comes in contact with the hot surface. A density gradient is thus generated and the lighter fluid is pushed upward due to buoyancy. The velocity at the wall is zero due to no slip. Thus the vertical velocity increases from zero to maximum and a hydrodynamic boundary layer is developed near the hot wall. The vertical velocity decreases towards the centre of the cavity because the density gradient is negligible in this region. An opposite effect is created at the cold wall i.e. the higher vertical velocity but in the downward direction. Similarly the horizontal velocities are high near the horizontal walls (figure 3(b)). The flow field inside the cavity is indicated using the contours of stream lines in figure 5. The streamlines obtained for Newtonian model (dashed lines) are superimposed over those obtained for non-Newtonian model (solid lines). The velocities are algebraically calculated by the spatial gradient of stream function values. Closely spaced streamlines near the wall indicate higher velocities while sparse stream lines indicate lower velocities. The temperature contours in the cavity for both Newtonian (dashed lines) and non-Newtonian model (solid lines) are shown in figure 4. The temperature at the core is constant due to almost zero absolute velocity at the core (figure 3(c)). When the heat transfer from the wall is high, the isotherms are almost horizontal at the core and become vertical in the thermal boundary layer region. Closely spaced isotherms indicate a very high temperature gradient near the wall and thus high heat transfer.

In the Newtonian model, viscosity is constant inside the cavity for a particular volume fraction. Increase in viscosity with volume fraction (ϕ) is accounted for here by the Brinkmann model. However there is also an increase in thermal conductivity with volume fraction which increases the diffusive heat flux. This leads to higher density gradients. All this leads to an overall increase in flow velocity with volume fraction (ϕ) for Newtonian model. This can be observed from figure 3(a) and 3(b) where the magnitude of horizontal and vertical centerline velocity increases with volume fraction for Newtonian model. Also in the streamline contours (shown by dashed-lines) of figure 5, as the volume fraction increases the value of innermost stream function decreases indicating an increase in velocity (the stream function value for the wall is zero here). With the increase in the velocity the thermal boundary layer decreases with ϕ (figure 3(c)) and the heat transfer by fluid from the wall increases. In figure 4, the isotherms are observed to get closer near the wall with increase in volume fraction (ϕ) indicating higher temperature gradient.

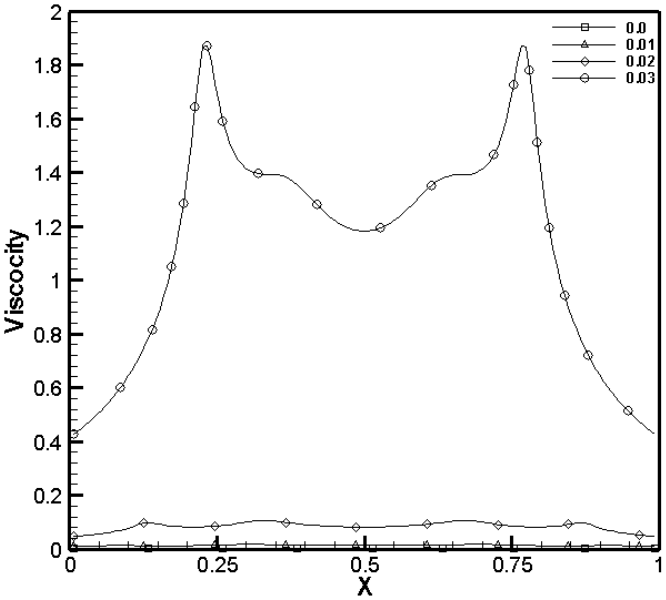

Fig. 6 Variation of viscosity with x at y = 0.5 at Ra = 10^6 for non-Newtonian model of nanofluid

For the Non-Newtonian model, the rise in viscosity is dependent on velocity gradient. The variation of viscosity inside the cavity for Non-Newtonian model is shown in figure 6 for different volume fractions. As the volume fraction increases; the viscosity also increases. This increase is much larger compared to Newtonian viscosity model. The value of viscosity for non-Newtonian model reaches to the order of 10^{-1} whereas when calculated by Brinkmann model (Newtonian approach) viscosity increase is of the order of 10^{-3} for ϕ < 5%. Thus when nanofluid is considered non-Newtonian, vertical and horizontal velocity is observed to decrease with increase in volume fraction which can be seen in figures 3(d) and 3(e). It can also be observed from figure 5 that for non-Newtonian model (values in bold) the value of innermost streamline tends to zero (the stream function value for the wall is zero here). This shows decrease in the flow with increase in volume fraction. The rise in thermal conductivity for non-Newtonian model is similar to Newtonian model for a particular volume fraction (ϕ) (there is some difference because thermal conductivity model includes effect of Brownian motion and thermal conductivity changes with temperature). However the effective heat transfer decreases with volume fraction (ϕ). This is

because the increase in viscosity and hence decrease in the velocity of flow has significantly larger influence than the increase in thermal conductivity. This degradation of effective heat transfer is also indicated by the isotherms in figure 4. As the value of volume fraction (ϕ) increases, the isotherms tend to become vertical in the central core region. This indicates increase in the thermal boundary layer and that the heat transfer is diffusion dominant. The spacing between the isotherms near the wall increases with volume fraction (ϕ) thereby indicating decrease in heat transfer. Thus it can be summarized that non-Newtonian model shows a deterioration in effective heat transfer coefficient with increase in volume fraction of nanofluid.

6.2 Influence of the Rayleigh number

For Newtonian model, the viscosity is dependent only on volume fraction (ϕ). For constant ϕ, the thermal conductivity remains almost constant (considering effect of temperature to be small). So the diffusion heat transfer will be same for all Rayleigh number (Ra). However the velocity of nanofluid increases with Ra as shown in figure 7(a) and 7(b). Thus convective heat transfer increases with Ra and thermal boundary layer decreases as is shown in figure 7(c). Also the nature of stream lines shown in figure 8 depicts that with the increase in Ra, the central vortex breaks into two parts and they move away from the centre of the cavity. This represents high velocities near the wall. The isotherms are densely packed near the wall for higher Ra as shown in figure 8. Thus, it is clear that effective heat transfer increases with the increase in Rayleigh number.

For the non-Newtonian model, the viscosity depends on the velocity gradient. With decrease of Ra, the flow velocities decrease (figure 7(a) and 7(b)). This increases the viscosity, which further resists the flow (figure 7(d)). Thus effectively, the convective heat transfer decreases. The decrease of effective heat transfer from wall with decrease in Ra is also shown by isotherms in figure 8. Heat transfer is maximum for Ra= 10^6 denoted by the closely spaced isotherms near the wall. Similar pattern is observed for the other values of volume fraction. Thus the effective decrease in heat transfer with decrease in Ra is more in case of non-Newtonian model.

6.3 Nusselt number variation

The relative strength of convective and conductive heat transfer is represented by Nusselt number. The variation of the Nusselt number along the hot wall for constant Ra= 10^6 and different values of ϕ is shown in figure 9. Figure 10 shows this variation with Rayleigh number for constant ϕ = 0.5%. The Nusselt number is high near bottom of the hot wall showing the maximum heat transfer at this place. This is because cold fluid coming in contact with the hot wall near the bottom has maximum heat absorption capacity. When this fluid goes up due to the buoyant force, its heat absorbing capacity decreases and hence the Nusselt number decreases.

From figure 9, it can be observed that for Newtonian model, maximum Nusselt number value tends to increase with ϕ indicating increase in heat transfer. For non-Newtonian model with the increase in ϕ the Nusselt number line tend to become vertical. This shows lower heat transfer (i.e. reduction in the convective heat transfer) near bottom. Figure 9 shows how drastically the Nusselt number falls with the decrease in the Rayleigh number for both Newtonian and non-Newtonian model.

Thus it can be summarized that for non-Newtonian model, with the increase in ϕ the shear rate decreases due to shear thinning behavior of the nanofluid. This causes a sharp rise in the viscosity and the magnitude of buoyancy driven flow decreases. Therefore the convective heat transfer decreases. The increase in the thermal conductivity is insufficient to recover this loss. On the contrary for Newtonian model, the viscosity increase is small and does not affect the convective flow and thus there is increase in heat transfer with increase in ϕ.

The variation of average Nusselt number for Newtonian (dashed-line) and non-Newtonian model is shown figure 11. For Newtonian model the average Nusselt number increases with volume fraction while it decreases with volume fraction for Non-Newtonian model drastically up to a volume fraction of 3%. This is true for the entire range of Rayleigh number considered here. It can be observed that the average Nusselt number increases by a fraction for non-Newtonian model for volume fraction beyond ϕ = 3% and Ra= 10^4 and 10^5. This can be attributed to the increase in diffusive heat transfer (thermal conductivity with volume fraction) and almost negligible heat transfer by convection for ϕ >3% (due to drastic increase of viscosity). However at Ra =10^6, there is decrease in average Nusselt number till ϕ =5% as the rise in viscosity is low at higher Rayleigh number.

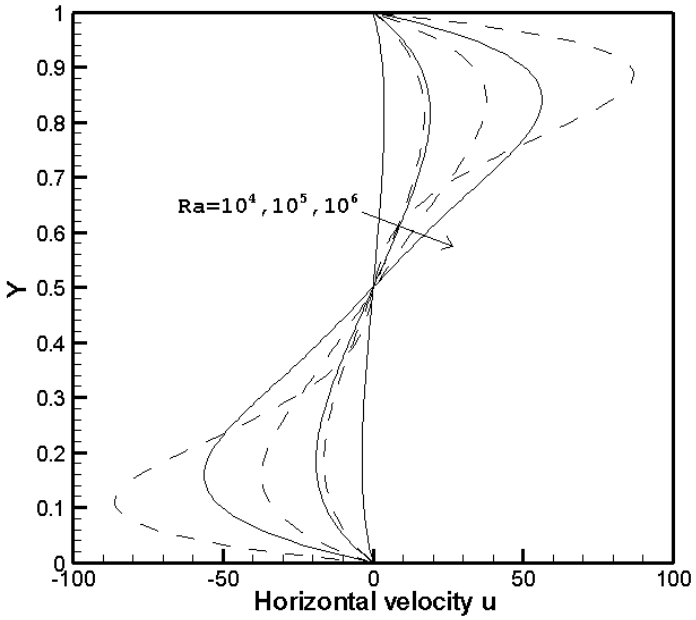

(a)

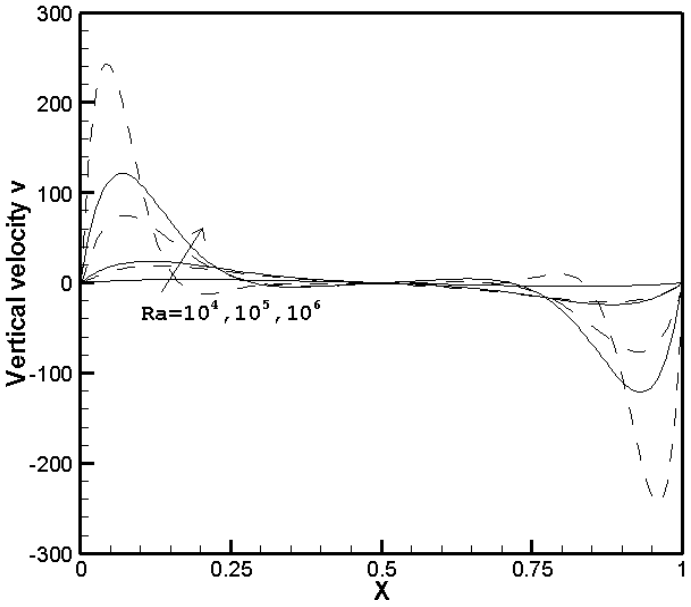

(b)

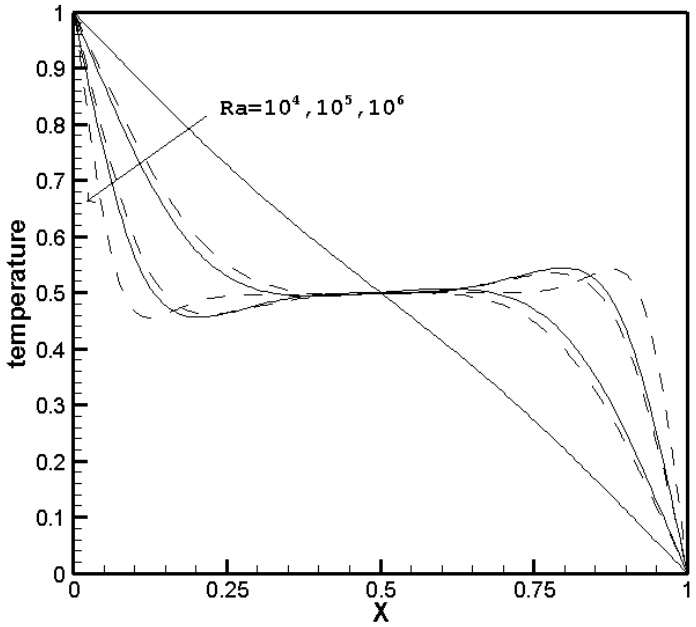

(c)

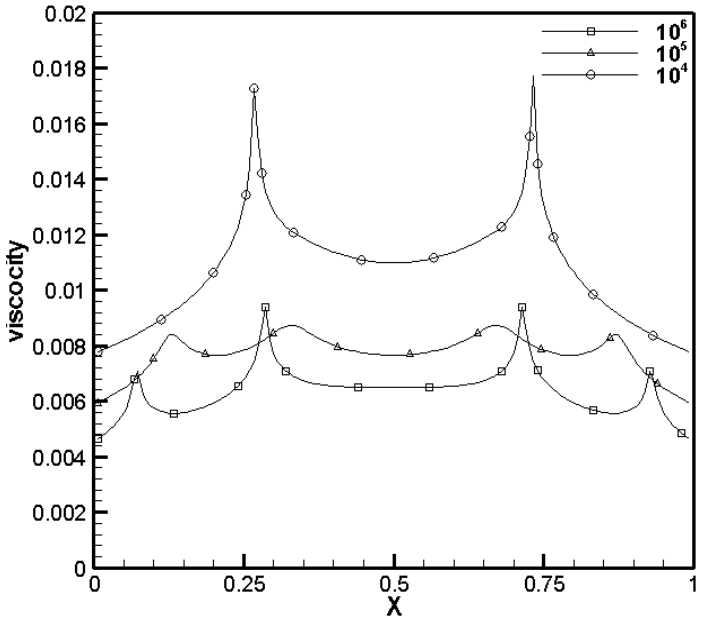

(d)

Fig. 7 Variation of (a) vertical velocity v with y at x= 0.5 (b) horizontal velocity (c) temperature and (d) viscosity with x at y = 0.5 at ϕ = 0.5% for Newtonian (dashed lines) and non-Newtonian nanofluid

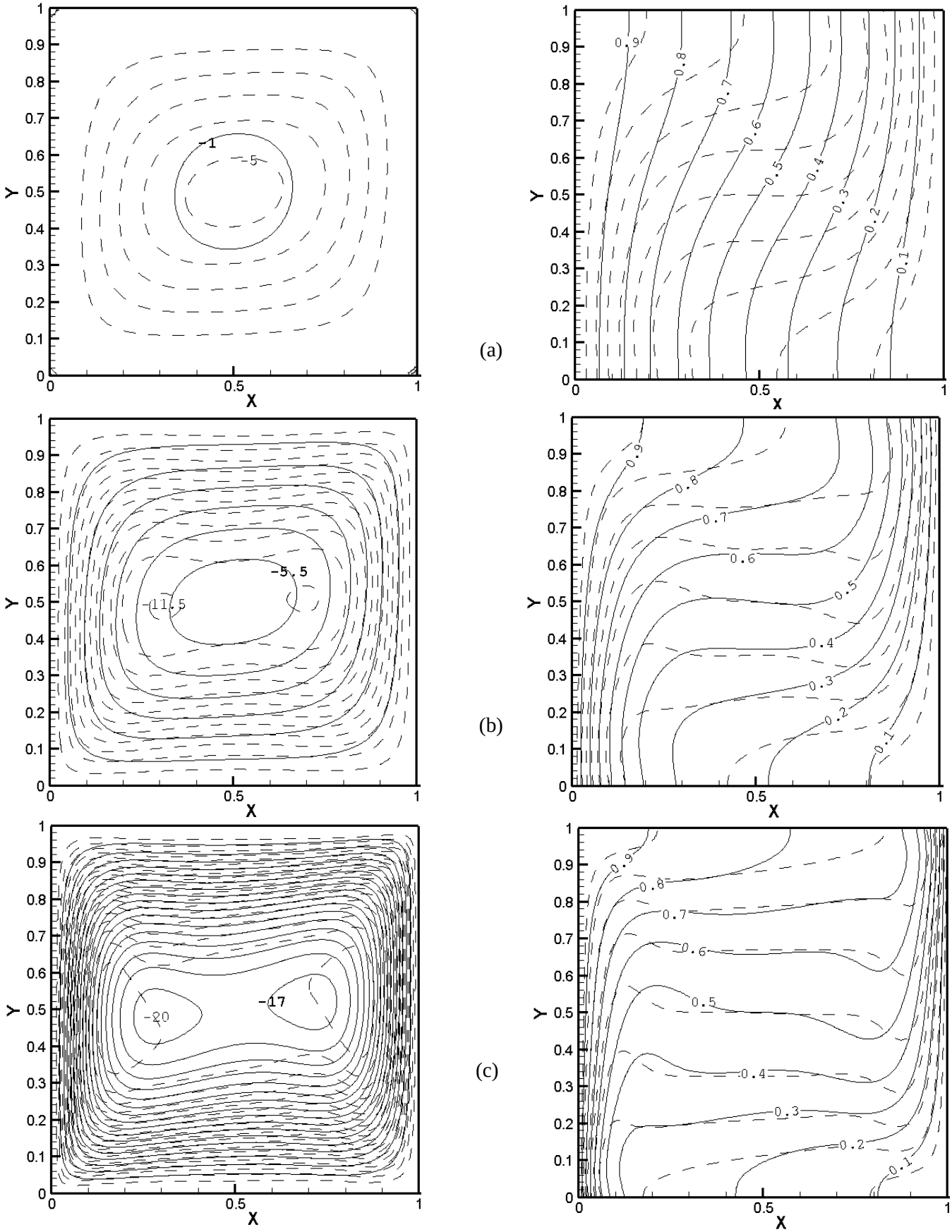

Fig. 8 Stream lines and isotherms for ϕ = 0.5% at (a) $Ra = 10^4$, (b) $Ra = 10^5$ and (c) $Ra = 10^6$ for Newtonian (dashed lines) and non-Newtonian nanofluid

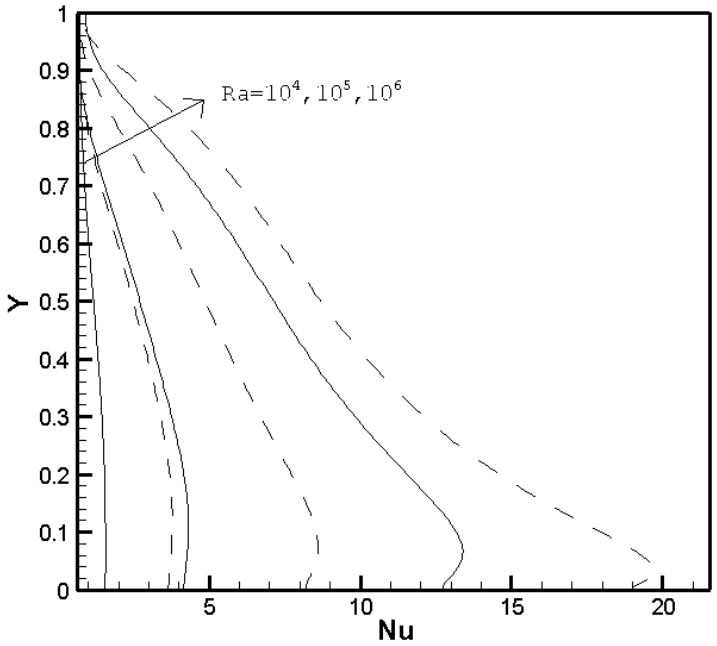

Fig. 9 Variation of Nusselt number along the hot wall for different ϕ and at $Ra = 10^6$ for Newtonian (dashed lines) and non-Newtonian nanofluid

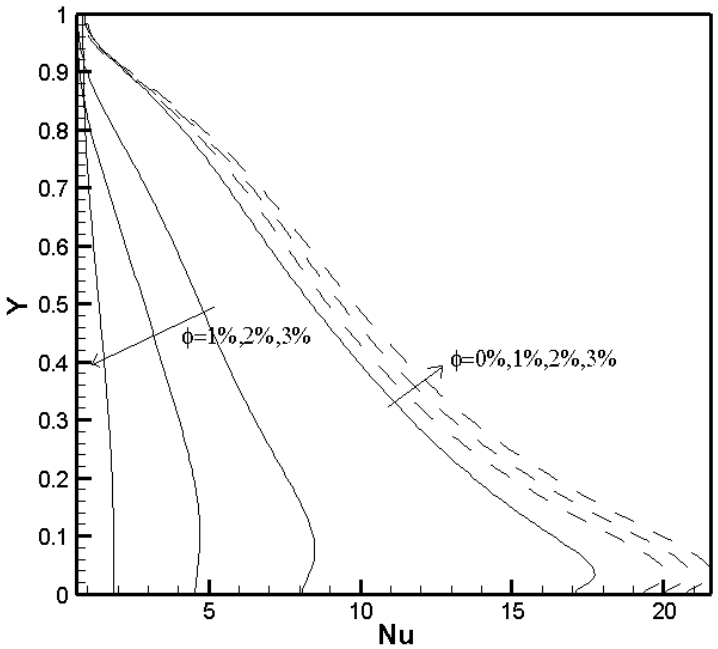

Fig. 10 Variation of Nusselt number along the hot wall at different *Ra* for $\phi = 0.5\%$ for Newtonian (dashed lines) and non-Newtonian nanofluid

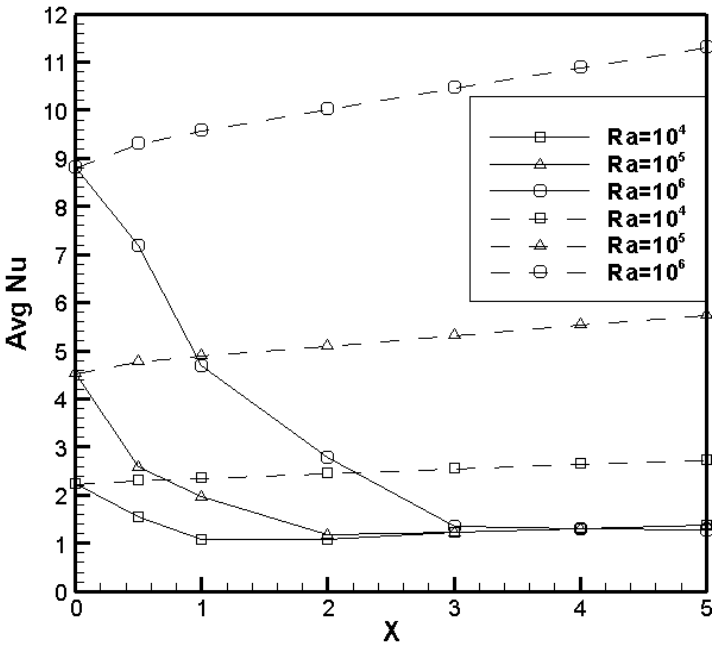

Fig. 11 Variation of average Nusselt number with ϕ at different *Ra* for Newtonian (dashed lines) and non-Newtonian nanofluid

7. Conclusion

A comparative analysis of natural convection is carried out for Newtonian and non-Newtonian models of nanofluid viscosity. The present numerical study shows a considerable decrease in heat transfer with increase in volume fraction of the suspended particles for non-Newtonian model and increase in the heat transfer for Newtonian model. This is observed for the entire range of Rayleigh number considered here. Thus it provides an insight on the influence of rhelogical behavior of nanofluid on heat transfer. Present work strongly emphasizes the need to systematically study the factors influencing the shear thinning behavior of nanofluids. This is because the shear thinning characteristics of nanofluid negates the very purpose of utility of nanofluid in heat transfer applications.

References:

[1] Penkavova V, Tihon J, Wein O, Stability and rheology of dilute TiO2-water nanofluids, *Nanoscale Res Lett*, Vol. 6, 2011, pp. 273.

[2] Namburua PK, Kulkarni DP, Misrab D, Das DK, Viscosity of copper oxide nanoparticles dispersed in ethylene glycol and water mixture, *Exp Therm Fluid Sci*, Vol. 32, 2007, pp. 397.

[3] Duan F, Kwek D, Crivoi A, Viscosity affected by nanoparticle aggregation in Al_2O_3-water

nanofluids, *Nanoscale Res Lett*, Vol. 6, 2011, pp. 248.

[4] Kulkarni DP, Das DK, Chukwu GA, Temperature dependent rheological property of copper oxide nanoparticles suspension (nanofluid), *J Nanosci Nanotechno*, Vol. 6, 2006, pp. 1150.

[5] Venerus *et al.*, Viscosity measurements on colloidal dispersions (nanofluids) for heat transfer applications, *Appl Rheol*, Vol. 20, 2010, pp. 44582.

[6] Chen H, Ding Y, Tan C, Rheological behaviour of nanofluids, *New J Phys*, Vol. 9, 2007, pp. 367.

[7] Chen H, Ding Y, Heat transfer and rheological behavior of nanofluids – A review. In: Wang L (ed) *Advances in Transport Phenomena*, Springer-Verlag Berlin Heidelberg, 2009, pp. 135.

[8] Santra AK, Sen S, Chakraborty N, Study of heat transfer due to laminar flow of copper–water nanofluid through two isothermally heated parallel plates, *Int J Therm Sci*, Vol. 48, 2009, pp. 391.

[9] Buongiorno J, Convective transport in nanofluids, *ASME J Heat Transf*, Vol. 128, 2006, 240.

[10] Koo J, Kleinstreuer C, Impact analysis of nanoparticle motion mechanisms on the thermal conductivity of nanofluids, *Int Commun Heat Mass*, Vol. 32, 2005, pp. 1111.

[11] Jang SP, Choi SUS, Role of Brownian motion in the enhanced thermal conductivity of nanofluids, *Appl Phys Lett*, Vol. 84, 2004, pp. 4316.

[12] Kumar DH, Patel HE, Kumar VRR, Sundararajan T, Pradeep T, Das SK, Model for Heat Conduction in Nanofluids, *Phys Rev Lett*, Vol. 93, 2004, pp. 144301.

[13] Keblinski P, Cahill DG, Comments on "Model for heat conduction in nanofluids", *Phys Rev Lett*, Vol. 95, 2005, pp. 209401.

[14] Patel HE, Sundararajan T, Pradeep T, Dasgupta A, Dasgupta N, Das SK, A micro-convection model for thermal conductivity of nanofluids, *Pramana J Phys*, Vol. 65, 2005, pp. 863.

[15] Kumar PCM, Kumar J, Sendhilnathan S, Theoretical model to determine the thermal conductivity of nanofluids, *Int J Eng Sci Tech*, Vol. 2, 2010, pp. 2846.

[16] Chandrsekar M, Suresh S, Srinivasan R, Bose AC, New analytical models to investigate thermal conductivity of nanofluids, *J Nanosci Nanotechno*, Vol. 9, 2009, pp. 533.

[17] Murshed SMS, Leong KC, Yang C, A combined model for the effective thermal conductivity of nanofluids, *Appl Therm Eng*, Vol. 29, 2009, pp. 2477.

[18] Xuan Y, Li Q, Heat transfer enhancement of nanofluids, *Int J Heat Fluid Fl*, Vol. 21, 2000, pp. 58.

[19] Brinkman H, The viscosity of concentrated suspensions and solutions, *J Chem Phys*, Vol. 20, 1952, pp. 571.

[20] Bird RB, Stewert WE, Lightfoot EN, *Transport Phenomena*, 2nd edn, Wiley, Singapore, 1960.

[21] Xuan Y, Roetzel W, Conceptions for heat transfer correlation of nanofluids, *Int J Heat Mass Tran*, Vol. 43, 2000, pp. 3701.

[22] Santra AK, Sen S, Chakraborty N, Study of heat transfer augmentation in a differentially heated square cavity using copper–water nanofluid, *Int J Therm Sci*, Vol. 47, 2008, pp. 1113.

[23] Putra N, Roetzel W, Das SK, Natural convection of nano-fluids, *Heat Mass Transfer*, Vol. 39, 2003, pp. 775.

[24] de Vahl Davis G, Natural convection of air in a square cavity - a benchmark numerical solution, *Int J Numer Meth Fl*, Vol. 3, 1962, pp. 249.

[25] Khanafer K, Vafai K, Lightstone M, Buoyancy-driven heat transfer enhancement in a two-dimensional enclosure utilizing nanofluids, *Int J Heat Mass Tran*, Vol. 46, 2003, pp. 3639.

[26] Fusegi T, Hyun JM, Kuwahara K, Farouk B, A numerical study of three-dimensional natural convection in a differentially heated cubical enclosure, *Int J Heat Mass Tran*, Vol. 34, 1991, pp. 1543.